



ELSEVIER

Contents lists available at ScienceDirect

Mechanical Systems and Signal Processing

journal homepage: www.elsevier.com/locate/ymssp

An optimization study for viscous dampers between adjacent buildings

Elif Cagda Kandemir-Mazanoglu ^{a,*}, Kemal Mazanoglu ^b^a Department of Civil Engineering, Usak University, 64200 Uşak, Turkey^b Department of Mechanical Engineering, Usak University, 64200 Uşak, Turkey

ARTICLE INFO

Article history:

Received 14 April 2016

Accepted 2 June 2016

Keywords:

Adjacent building
Structural pounding
Viscous damper
Seismic behavior
Optimization

ABSTRACT

This paper investigates optimum viscous damper capacity and number for prevention of one-sided structural pounding between two adjacent buildings under earthquake motion. The buildings assumed as shear-type structures are modeled by using lumped mass-stiffness technique. Impact forces due to pounding is simulated by nonlinear elastic spring approximation called Hertz model. A parametric study is conducted by varying storey number and stiffness of buildings in addition to the capacity of the viscous dampers. Pounding force and supplemental damping ratio for each case are presented based upon newly defined nondimensional natural frequency parameter ratio. An optimization procedure for determination of viscous damper capacity is developed based on modified supplemental damping ratio equation. Results are compared with each other to clarify the effect of variation in building parameters on pounding forces and viscous damper capacity.

© 2016 Elsevier Ltd. All rights reserved.

1. Introduction

Buildings in metropolitan cities are usually constructed close to each other due to scarcity of land in densely populated areas like city centers. The seismic gaps stipulated in seismic design codes allow the neighboring buildings and structural parts to make relative translational movements without collision during earthquakes. However, insufficient gap between buildings subjected to ground motions may cause structural pounding leading to significant damages or even collapse as experienced in past earthquakes such as 1985 Mexico City and 1989 Loma Prieta earthquakes [1–4]. Main reason of the earthquake-induced structural pounding is out-of-phase behavior between neighboring buildings due to having different dynamic characteristics. To overcome this problem, there are a number of solutions applied in practice and also proposed in the related literature. The connection of the buildings by linking devices is the most common method used for prevention of pounding. Xu et al. [5] applied fluid viscous damper between adjacent buildings with different number of storeys. The analyses were done in both frequency and time domain to show the efficiency of dampers. Bhaskararao and Jangid [6] implemented friction dampers to reduce seismic responses of adjacent buildings. Raheem [7] used rubber shock absorber to avoid pounding. Yang et al. [8] performed an experimental seismic study of adjacent buildings with fluid dampers. Basili and De Angelis [9] studied the optimal passive control of adjacent structures interconnected by Bouc-Wen model nonlinear hysteretic devices under seismic excitations of a Gaussian zero mean white noise and a filtered white noise. Kim et al. [10]

* Corresponding author.

E-mail address: elif.kandemir@usak.edu.tr (E.C. Kandemir-Mazanoglu).

analyzed the single degree-of-freedom (SDOF) systems connected by viscoelastic dampers at the seismic joints, under white noise and earthquake ground excitations, in order to observe reduction in earthquake-induced structural responses. They also performed dynamic analyses for 5-storey and 25-storey rigid frames connected to braced-frames. Kandemir-Mazanoglu and Mazanoglu [11] developed a simple optimization procedure for determination of capacity and location of linear viscous dampers between adjacent buildings. They conducted parametric study on both equal and stiff buildings connected with each other by linear viscous damper devices.

In this paper, two adjacent buildings with floors in alignment are analyzed through ground motion, 1999 Duzce earthquake (PGA 239.5 gal), to observe earthquake-induced structural pounding. To the best of author's knowledge, parametric study including location and capacity optimization of viscous dampers to prevent pounding is scarce and/or complex in current literature. In this study, various structural characteristics are taken into account by changing storey numbers and stiffness of buildings. The effects on pounding force are investigated for the cases of varied storey number of equal, stiffer and flexible buildings. Seismic time responses, i.e. displacement and impact forces, are obtained via Newmark- β method. The impact forces between adjacent buildings modeled as nonlinear elastic spring are analyzed for three cases considered. An optimization procedure for prevention of pounding effect by linear and nonlinear viscous dampers is carried out in order to find out optimum location and capacity of dampers. The aim in computation of nonlinear viscous damper capacity is to observe capacity reduction in comparison with that of linear viscous damper. The command of *fmincon* in Matlab Optimization Toolbox is used for optimization of viscous damper capacity and location. The boundary and equality constraints of optimization problem are constituted based on modified formulation of the supplemental damping ratio formulation proposed by FEMA 273/356 [12,13].

2. Formulations

2.1. Viscous dampers

Viscous dampers are velocity-dependent passive energy dissipation devices which do not possess inherent rigidity. Fig. 1 (a) shows schematic of a typical viscous damper. Piston moves with the movement of structure during earthquake motion forcing the viscous fluid inside cylinder to be passed through orifices on piston head. Dissipation of seismic energy is executed by transformation of kinetic energy into heat energy. Displacement response control of these devices is dependent on the stroke of the damper. Inside the stroke limit, viscous damper has no inherent stiffness. The produced damper force F_d , given in Eq. (1), depends on relative velocity between damper ends as follows;

$$F_d = cd(\alpha) |\dot{x}|^\alpha \operatorname{sgn}(\dot{x}) \quad (1)$$

where $cd(\alpha)$ is damping coefficient which depends on velocity exponent α , \dot{x} is relative velocity between damper ends, sgn is signum function. Velocity exponent takes value between 0 and 1. This constant value designates the damper type. The device is friction type, linear viscous and nonlinear viscous damper for $\alpha=0$, $\alpha=1$ and for $0 < \alpha < 1$, respectively. Fig. 1(b) depicts the force-displacement characteristics of three types of dampers. It is worth noting that damper force of NVD is less than that of LVD for same relative velocity response due to velocity exponent less than one. This feature saves the device from excessive forces when high velocity response occurs. Both linear and nonlinear viscous dampers are addressed in this paper to find out the effects of parametric changes on capacity reduction. Equation of motion of a single degree-of-freedom system with viscous dampers subjected to ground motion is written as in Eq. (2),

$$m\ddot{x}(t) + c\dot{x}(t) + kx(t) + cd(\alpha)\dot{x}(t) = -m\ddot{x}_g(t) \quad (2)$$

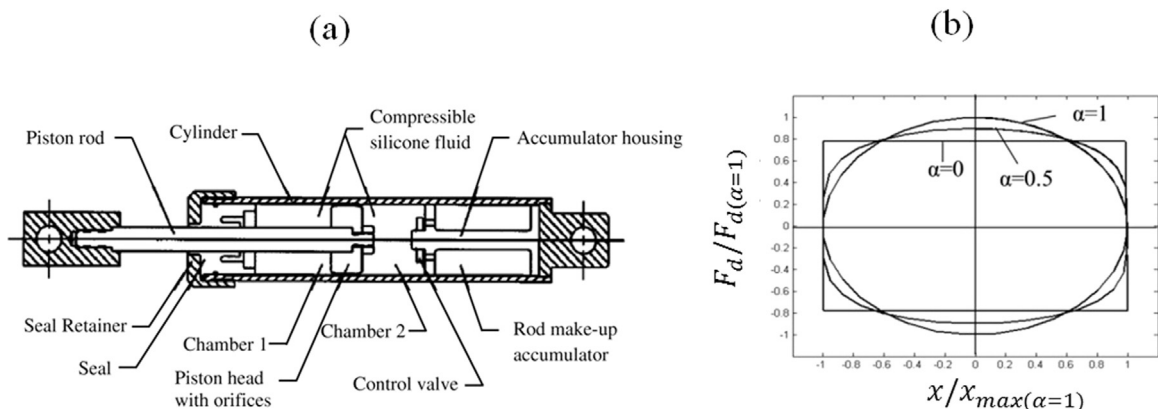


Fig. 1. (a) Schematic view (Symans and Constantinou, [14]) and (b) force-displacement relation of friction, linear and nonlinear viscous damper.

in which m is mass, k is stiffness, c is inherent damping coefficient and \ddot{x}_g is the acceleration of ground motion. $x(t)$ is displacement response at time t and overdots symbolize the differentiation with respect to time. The damping ratio added to the system by LVDs is given by Eq. (3) [12,13],

$$\xi_d = \frac{T_1 \sum_j cd(\alpha)_j \cos^2(\theta_j) (\phi_j - \phi_{j-1})^2}{4\pi \sum_i m_i \phi_i^2} \tag{3}$$

where T_1 is fundamental natural period, θ_j is inclination angle of damper, ϕ is 1st mode horizontal modal displacement, m is mass of one floor. Subscript i is used for indexing the floor while j is the floor where the dampers added. In this study viscous dampers are installed between adjacent floors of two buildings, therefore, Eq. (3) is modified as follows,

$$\xi_d = \frac{(\max\{T_{1,1}, T_{1,2}\}) \sum_j cd(\alpha)_j (\phi_{j,1} - \phi_{j,2})^2}{4\pi \sum_i m_i \phi_i^2} \tag{4}$$

where $\max\{T_{1,1}, T_{1,2}\}$ denotes the largest period among the first natural periods of two buildings and subscripts after comma denote the building number. Since the dampers are considered to be placed in horizontal direction to the same floor number of two buildings, θ is zero in Eq. (4). $(\phi_{j,1} - \phi_{j,2})$ indicates the relative horizontal modal displacements between adjacent floors of two buildings.

By the assumption of energy dissipation equivalence of LVD to NVD in one cycle of force-displacement diagram, NVD capacity can easily be calculated. The relation between NVD coefficient and LVD coefficient is given by,

$$cd(\alpha) = \frac{cd(1) (\min\{\omega_{1,1}, \omega_{1,2}\} \cdot x_0)^{1-\alpha}}{\beta} \tag{5}$$

where $cd(1)$ is damper coefficient of LVD, $\min\{\omega_{1,1}, \omega_{1,2}\}$ is the smallest natural frequency among the first natural frequencies of two buildings, x_0 is maximum relative displacement response between adjacent floors and the constant β is formulated as follows;

$$\beta = \frac{2^{2+\alpha} \Gamma^2(1 + \alpha/2)}{\pi \Gamma(2 + \alpha)} \tag{6}$$

where Γ is the gamma function.

2.2. Analytical impact model

The impact force between adjacent structures can be modeled with various analytical models such as nonlinear elastic, linear viscoelastic, and nonlinear viscoelastic models (see Reference [15]). In this paper only nonlinear elastic model, called as the Hertz model, has been used for simplicity. This model neglects the plastic deformations during pounding and assumes that the nonlinear elastic spring become active when the gap between buildings (a) is closed. The analytical impact model of adjacent single degree-of-freedom systems is given in Fig. 2.

Pounding force is calculated by the formulation below;

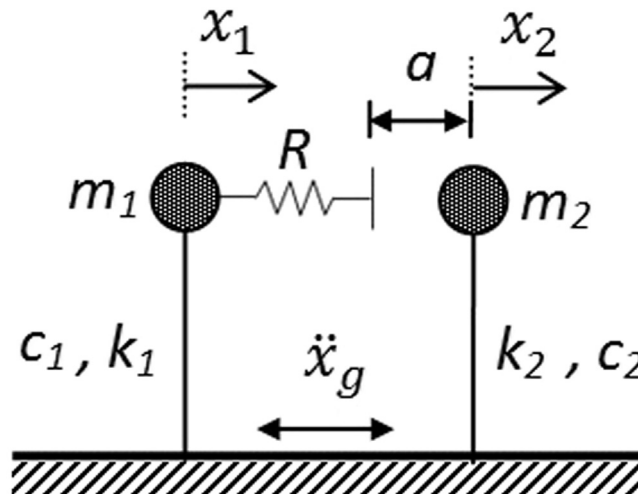


Fig. 2. Analytical impact model.

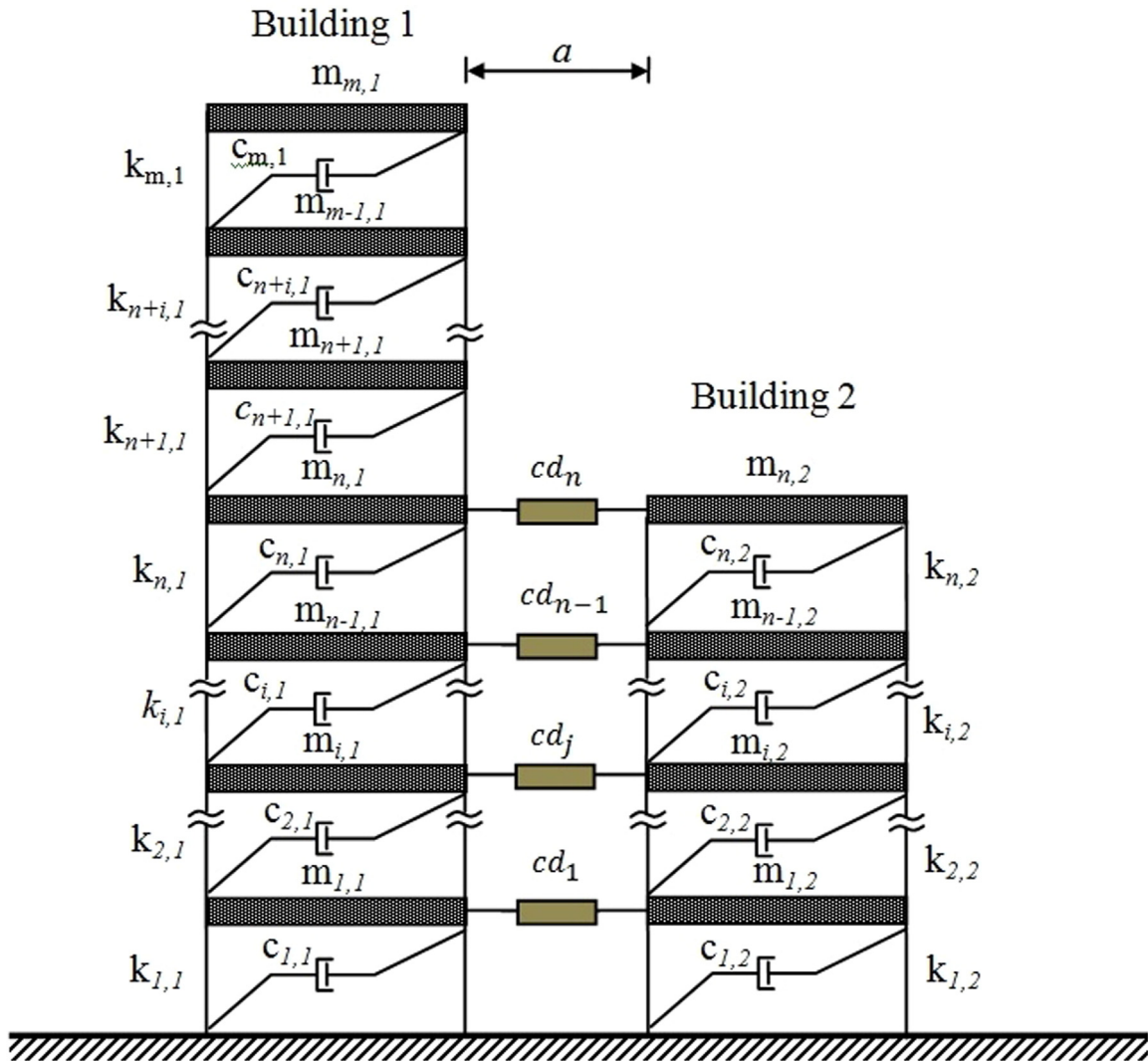


Fig. 3. Configuration of adjacent buildings.

$$F_p(t) = \begin{cases} R\delta(t)^{3/2}, & \delta(t) \geq 0 \\ 0, & \delta(t) < 0 \end{cases} \quad (7)$$

$$\delta(t) = x_1(t) - x_2(t) - a \quad (8)$$

where the force, F_p , is simply calculated as restoring force of the elastic spring with an exponential expression of relative displacement value, δ . R indicates constant stiffness coefficient of the spring. It takes between $40 \text{ kN/mm}^{3/2}$ and $80 \text{ kN/mm}^{3/2}$ ($1.2 \times 10^9 - 2.6 \times 10^9 \text{ N/m}^{3/2}$) according to experimental analyses conducted on concrete surfaces [16].

2.3. Equations of motion of buildings connected with viscous dampers

Building 1 and 2 are m -storey and n -storey adjacent buildings, respectively. Fig. 3 shows buildings connected at each neighboring floor level by viscous dampers. The mass, stiffness and damping coefficients of building 1 and building 2 are $m_{i,1}$, $k_{i,1}$, $c_{i,1}$ and $m_{i,2}$, $k_{i,2}$, $c_{i,2}$, respectively. The damper coefficient of viscous damper at the j th floor is denoted by cd_j .

Equation of motion of two linked buildings with linear viscous dampers is given as,

$$\mathbf{M}\ddot{\mathbf{X}} + (\mathbf{C} + \mathbf{Cd})\dot{\mathbf{X}} + \mathbf{KX} + \mathbf{F}_p = -\mathbf{Mr}\ddot{x}_g \quad (9)$$

where \mathbf{M} , \mathbf{K} and \mathbf{C} are mass, stiffness and damping matrices with the size of $m+n$. \mathbf{r} is influence coefficient matrix in the

form of unit vector. Eqs. (10a) and (10b) shows detailed structural matrices and damping coefficient matrix (\mathbf{Cd}) of linear viscous dampers, respectively, as follow,

$$\mathbf{M}_{(m+n, m+n)} = \begin{bmatrix} [\mathbf{M}_1] & [0] \\ (m, m) & (m, n) \\ [0] & [\mathbf{M}_2] \\ (n, m) & (n, n) \end{bmatrix} \quad \mathbf{K}_{(m+n, m+n)} = \begin{bmatrix} [\mathbf{K}_1] & [0] \\ (m, m) & (m, n) \\ [0] & [\mathbf{K}_2] \\ (n, m) & (n, n) \end{bmatrix} \quad \mathbf{C}_{(m+n, m+n)} = \begin{bmatrix} [\mathbf{C}_1] & [0] \\ (m, m) & (m, n) \\ [0] & [\mathbf{C}_2] \\ (n, m) & (n, n) \end{bmatrix} \quad (10a)$$

$$\mathbf{Cd}_{(m+n, m+n)} = \begin{bmatrix} [\mathbf{A}] & [0] & [-\mathbf{A}] \\ (n, n) & (n, m-n) & (n, n) \\ [0] & [0] & [0] \\ (m-n, n) & (m-n, m-n) & (m-n, n) \\ [\mathbf{A}] & [0] & [-\mathbf{A}] \\ (n, n) & (n, m-n) & (n, n) \end{bmatrix} \quad (10b)$$

where subscripts, 1 and 2, denote the building numbers. In supplemental viscous damper coefficient matrix, \mathbf{Cd} , $[\mathbf{A}] = \text{diag}(cd)$ and $[-\mathbf{A}] = \text{diag}(-cd)$. Damper coefficient vector, i.e. $cd = \{cd_1, \dots, cd_j, \dots, cd_n\}$, is a vector with the size of storey number of building 2, n .

2.4. Optimization procedure of viscous damper capacity and location

The major purpose of this study is to obtain adequate capacity and ideal locations of viscous dampers for prevention of structural pounding. Optimization function, f , given in Eq. (11), is considered to minimize total damper capacity attached between adjacent floors.

$$\text{Min } f = \sum_{j=1}^n cd_j \quad (11)$$

Optimization problem has lower and upper bounds to constraint damper capacity. Lower bound, lb , is assigned to zero to represent the case of no damper placed between the buildings. Upper bound, i.e. predefined maximum capacity, ub , can take arbitrary values. Equality constraint is derived based upon supplemental damping ratio formulation in Eq. (4) extracting the unknown LVD coefficient term as follow,

$$A_{eq(j)} = \frac{(\max\{T_{1,1}, T_{1,2}\})}{4\pi \sum_{i=1}^{m+n} m_i \phi_i^2} (\phi_{j,1} - \phi_{j,2})^2 \quad (12)$$

$$\{\mathbf{A}_{eq}\} = \{A_{eq,1}, \dots, A_{eq,j}, \dots, A_{eq,n}\} \quad (13)$$

$$\{\mathbf{A}_{eq}\}[\mathbf{cd}] = \xi_d \quad (14)$$

$\{\mathbf{A}_{eq}\}$ is a row vector including n terms whereas $[\mathbf{cd}]$ is a column vector with same number of terms. Their multiplication gives supplemental damping ratio, ξ_d . In optimization algorithm, cd values are calculated between lower and upper bounds for each step of gradually increased ξ_d . The computed damper capacity vector is correctly placed into Eq. (10b).

The procedure for placement optimization for dampers starts to connect adjacent floors from top of the building 2 where the maximum pounding force occurs. Capacities of dampers to be placed are totally dependent on the upper bound value. At first, the algorithm states the damper with upper bound capacity to the top neighboring floor. Then, if the first damper is inadequate to avoid structural pounding, second damper with required capacity is placed to the lower floor.

3. Results and discussion

In this paper some assumptions are necessary to present parametric study results in a convenient way and to highlight the efficiency of viscous damper optimization algorithm. Two buildings are considered as symmetric in plan and the ground motion is assumed to be subjected in one direction so that two dimensional configuration is adequate to conduct response analyses. The buildings are shear-type linear multi degree-of-freedom (MDOF) systems. The floors are in alignment and equal in height. The mass, stiffness and inherent damping coefficient are equally distributed among floors. The impact forces occur only on the floor levels and plastic deformations during pounding are neglected. Since the pounding issue is not the core of this study, the simplest nonlinear spring model is chosen for simulation of pounding force.

The results are given for three cases considered: Case 1 includes two buildings with the same mass and stiffness for each storey as $m_{i,1} = m_{i,2} = 1 \times 10^5$ kg and $k_{i,1} = k_{i,2} = 6.8 \times 10^7$ N/m, respectively. In Case 2, second building is stiffer with $k_{i,2} = 10 \times 10^8$ N/m. In Case 3, second building is more flexible with $k_{i,2} = 7.2 \times 10^6$ N/m. All cases are carried out for storey

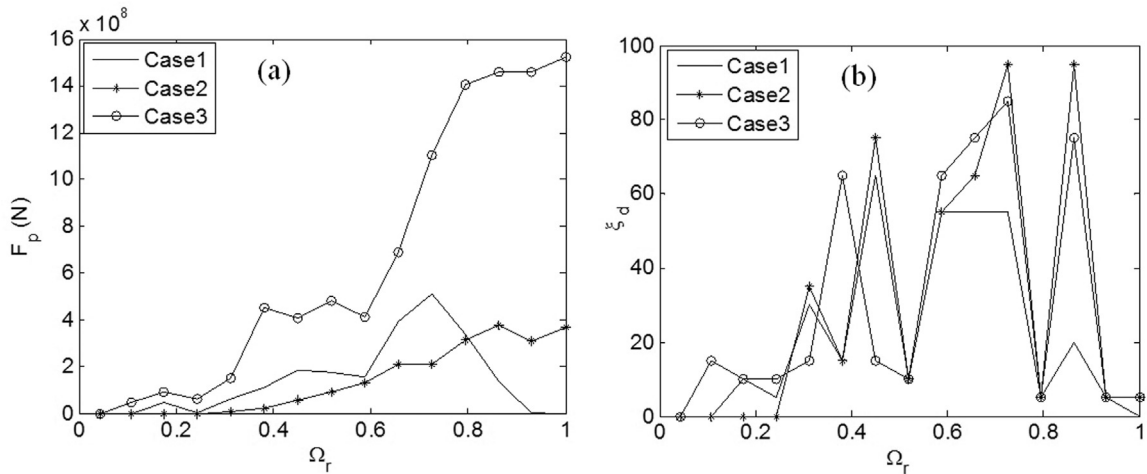


Fig. 4. Relation between nondimensional frequency ratio parameter (Ω_r) and (a) pounding force (b) supplemental damping ratio (ξ_d).

numbers of building 2 varied from 1 to 15 while storey number of building 1 is kept constant as 15. The inherent damping ratio (ξ) is 5% for both buildings and Rayleigh damping is used for constitution of damping matrix. The seismic gap a , is assigned to be 0.16 m which is calculated based on provision (2.10.3.2) of Turkish Earthquake Code 2007 [17]. The spring constant in Hertz model for pounding force is assumed as $80 \text{ kN/mm}^{3/2}$. In this study, in addition to linear viscous dampers, nonlinear viscous dampers with velocity exponent of 0.5 are also taken into account to observe the capacity reduction.

3.1. Natural period based variation of impact force and supplemental damping ratio

Different vibration characteristics of closely located adjacent buildings under ground motions result in out-of-phase behavior which is the main reason of earthquake-induced structural pounding. In this section three cases are investigated in order to observe the effect of natural frequency differences of buildings on the impact force. The cases are compared with each other in a nondimensional scale developed in this study, instead of natural frequency ratio ($\omega_{1,1}/\omega_{1,2}$) which varies with changing characteristics of each building. Nondimensional frequency parameter (Ω) is defined as follows;

$$\Omega = \omega_1 s^2 \sqrt{\frac{m}{k}} \tag{15}$$

in which ω_1 is the natural frequency of the buildings, s is storey number, m and k are mass and stiffness coefficient of one floor. Effects of the ratio between nondimensional natural frequencies ($\Omega_r = \Omega_2/\Omega_1$) of adjacent buildings on pounding force are depicted in Fig. 4(a). The pounding force increases as one of the buildings gets more flexible and it tends to get larger

Table 1

Total damper coefficients of linear (LVD) and nonlinear viscous dampers (NVD) for corresponding required supplemental damping ratio in Case 1, 2 and 3. (B1: Building 1, B2: Building 2).

Storeys of B1/B2	Ω_r	Total damper coefficient ($\times 10^5 \text{ Ns/m}$)								
		Case 1			Case 2			Case 3		
		ξ_d (%)	LVD	NVD (reduction %)	ξ_d (%)	LVD	NVD (reduction %)	ξ_d (%)	LVD	NVD (reduction %)
15/01	0.0439	-	-	-	-	-	-	-	-	-
15/02	0.1085	-	-	-	-	-	-	15	2.62	1.41 (46.2)
15/03	0.1757	10	2.70	1.61 (40.4)	-	-	-	10	2.67	1.52 (43.1)
15/04	0.2438	5	1.99	1.30 (34.7)	-	-	-	10	3.99	2.15 (46.1)
15/05	0.3112	30	5.41	3.72 (31.2)	35	6.52	3.72 (42.9)	15	2.44	1.42 (41.8)
15/06	0.3808	15	13.99	8.59 (38.6)	15	13.99	7.77 (44.5)	10	6.87	3.45 (49.8)
15/07	0.4494	65	14.27	8.83 (38.1)	75	17.81	10.25 (42.4)	65	8.75	5.07 (42.1)
15/08	0.5182	10	21.45	11.96 (44.2)	10	21.45	12.23 (43.0)	15	18.51	9.27 (49.9)
15/09	0.5870	55	11.35	7.33 (35.4)	55	11.35	7.68 (32.3)	65	13.82	8.10 (41.4)
15/10	0.6558	55	11.25	7.32 (34.9)	65	13.63	8.83 (35.2)	75	16.19	9.45 (41.6)
15/11	0.7246	55	11.18	6.86 (38.6)	95	21.48	13.06 (39.2)	85	18.57	10.78 (41.9)
15/12	0.7934	5	138.92	26.58 (80.9)	5	138.92	46.86 (66.3)	5	138.92	42.35 (69.5)
15/13	0.8623	20	3.94	2.25 (42.9)	95	18.73	12.77 (31.8)	75	15.68	10.19 (35)
15/14	0.9311	5	1579.10	37.07 (97.6)	5	1579.10	211.3 (86.6)	5	1579.10	177.73 (88.7)
15/15	1	-	-	-	5	45.00	21.08 (53.2)	5	45.00	21.43 (52.4)

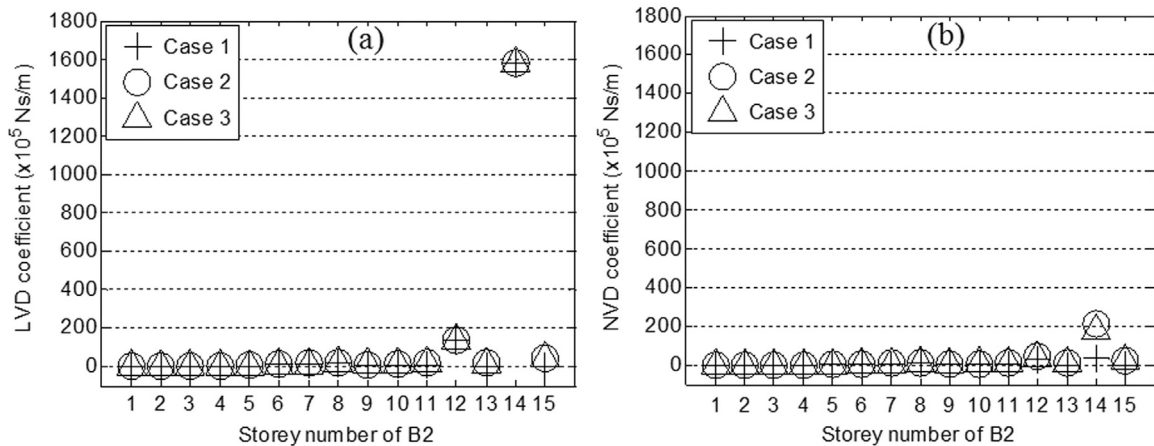


Fig. 5. Total capacities of (a) linear and (b) nonlinear viscous dampers with varied storey number of building 2.

with ascending nondimensional natural frequency ratio except for Case 1. The reason is that in-phase behavior is promptly obtained in Case 1 once the storey numbers of two buildings become equal. As a result of being more flexible in Case 3, building 2 displaces larger than other cases leading to larger pounding force for each nondimensional frequency ratio. In Case 2, since building 2 is stiffer, less pounding force is observed. Fig. 4(b) presents natural frequency ratio versus supplemental damping ratios required to vanish pounding force. The required damping ratios are supplied to inherent damping ratio by means of viscous dampers. From Fig. 4(a) and (b), it is clear that required damping ratios are independent from pounding force value, however, interestingly show similar behavior in all cases.

Table 1 presents damping ratios required in each case and corresponding total damper coefficient of LVDs and NVDs for the upper bound value of 5×10^5 Ns/m. The results show that the largest supplemental damping ratios are needed in Case 2 and 3 when the building 2 has 11 and 13 storeys. Total damper coefficients of LVD and NVD for varied storey number of building 2 are depicted in Fig. 5(a) and (b), respectively. There is a clear jump in capacity of both dampers when building 2 has 14 storeys. In all cases, required total NVD capacity is less than total LVD capacity when the Table 1 and Fig. 5 are compared. Maximum capacity reductions are obtained when building 2 has 14 storeys. The largest reduction occurs in Case 1 by 97.6%. There are both advantages and disadvantages in usage of NVDs. They are not cost-effective, however, saves the device from large damper forces during excessive velocities as mentioned before.

Displacement time responses of top floors are given in Figs. 6–8 to clarify the displacement reduction and in-phase behavior after implementation of dampers. The cases for 15/14 storey scenarios are presented since required damper capacities are largest in these scenarios. Before connection by viscous dampers, displacement responses of the structures intersect with each other at the time when pounding occurs. After installation, the structures displace in-phase and seismic responses decrease for both buildings.

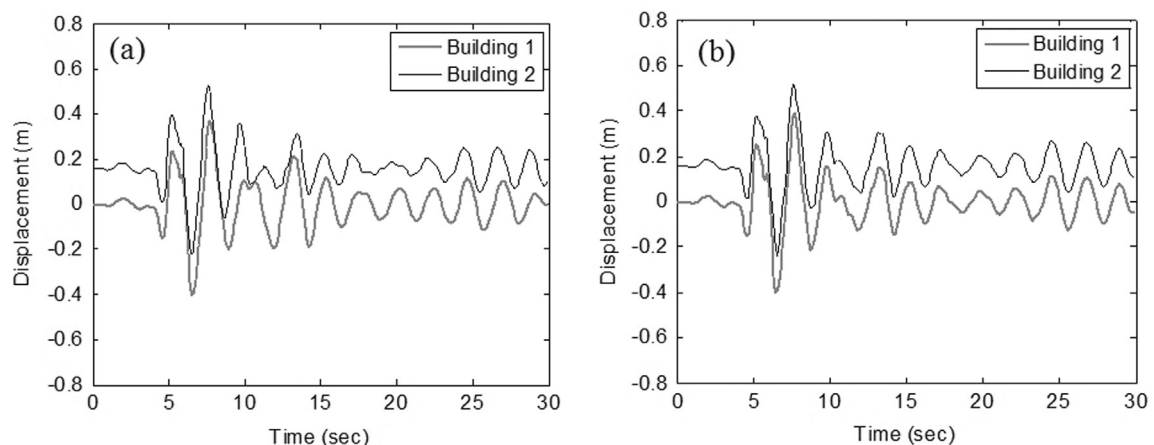


Fig. 6. Case 1 for 15/14 scenarios (a) without dampers (b) with dampers.

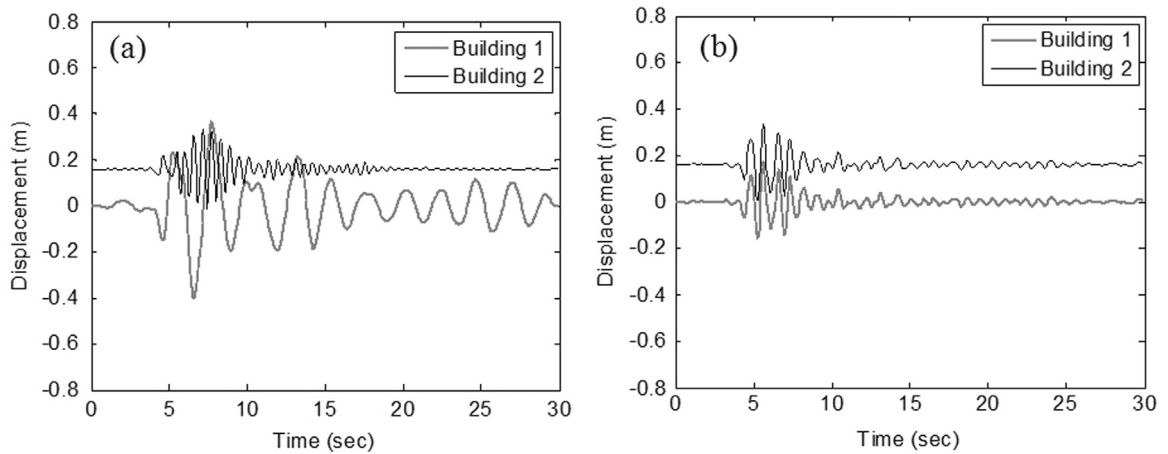


Fig. 7. Case 2 for 15/14 scenarios (a) without dampers (b) with dampers.

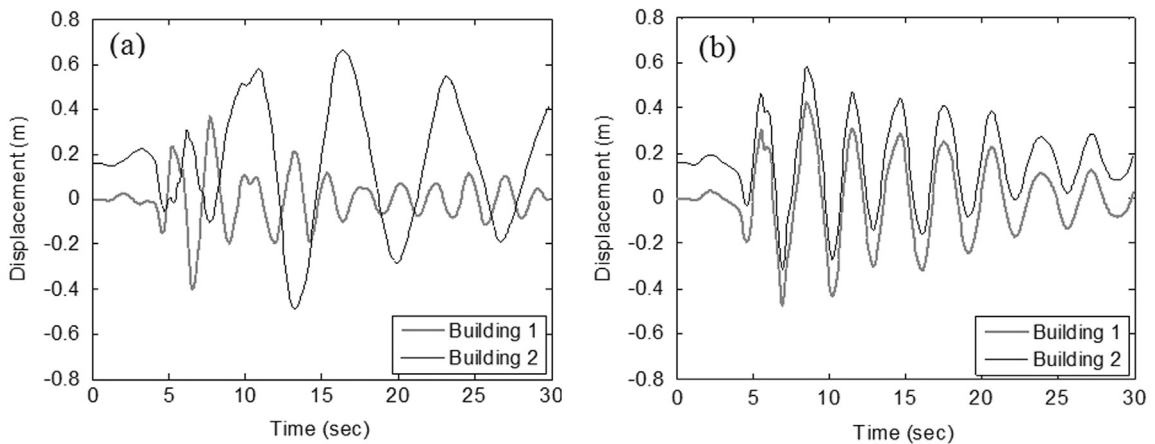


Fig. 8. Case 3 for 15/14 scenarios (a) without dampers (b) with dampers.

3.2. Placement optimization of viscous dampers

In the location algorithm, the damper capacity attached between an adjacent floor depends on upper bound. Results for 11 and 10 storey scenarios in Case 1 are given in Table 2. It is clear that the optimization algorithm starts to locate dampers

Table 2

Floors to be connected with dampers and total capacities for different upper bound values for 15/11 and 15/10 scenarios in Case 1.

Adjacent floor no.	Upper bound for damper capacity (ub) ($\times 10^5$ Ns/m)							
	50.00		10.00		3.00		1.00	
	15/11	15/10	15/11	15/10	15/11	15/10	15/11	15/10
11	10.65	-	10.00	-	3	-	2.16	-
10	-	10.61	0.70	10.00	3	3	2.16	2.56
9	-	-	-	0.66	3	3	2.16	2.56
8	-	-	-	-	3	3	2.16	2.56
7	-	-	-	-	1.84	3	2.16	2.56
6	-	-	-	-	-	2.44	2.16	2.56
5	-	-	-	-	-	-	2.16	2.56
4	-	-	-	-	-	-	2.16	2.56
3	-	-	-	-	-	-	2.16	2.56
2	-	-	-	-	-	-	2.16	2.56
1	-	-	-	-	-	-	2.16	2.56
Σ	10.65	10.61	10.70	10.66	13.85	14.44	23.74	25.63

from the top adjacent floors. Table 2 also demonstrates that the number of damper device to be installed decreases as upper bound value increases. When the upper bound value is kept small, number of neighboring floors connected by viscous dampers as well as total damper capacity increases. These results validate the previous explanations mentioned in subsection 2.4. The decision about the damper capacity and number of damper device should be given by the designer and the manufacturer together in the aspect of economical and functional conditions.

4. Conclusion

In this paper, the optimization procedure to obtain capacity and location of viscous dampers connecting adjacent buildings has been explained. Different vibration characteristics of neighboring buildings result in structural pounding which may lead to harmful damages. Variations of pounding force and supplemental damping ratio are represented based upon nondimensional scale of natural frequencies which is developed to be able to compare the cases including buildings with different structural characteristics. It is obtained that pounding force mainly rely on structural characteristics of buildings. In addition, it is concluded that supplemental damping ratio for prevention of pounding is not proportional with pounding forces.

In this paper, the existing design formula of structures with supplemental viscous dampers has been modified for two buildings connected by viscous dampers. The results show that optimum selection of damper properties reduces displacement responses effectively and prevents pounding.

The relation between upper bound of damper capacity, total damper capacity and the number of damper devices is achieved by the optimization algorithm for placement of damper devices. Ascending upper bound decreases both total capacity and number of dampers and vice versa.

This paper contributes to related literature in terms of effective and simplified solution to overcome structural pounding problem.

References

- [1] A. Moustafa, S. Mahmoud, Damage assessment of adjacent buildings under earthquake loads, *Eng. Struct.* 61 (2014) 153–165.
- [2] S. Naserkhaki, F.N.A. Abdul Aziz, H. Pourmohammad, Earthquake induced pounding between adjacent buildings considering soil-structure interaction, *Earthq. Eng. Eng. Vib.* 11 (2012) 343–358.
- [3] E. Rosenblueth, R. Meli, The 1985 Earthquake: Causes and effects in Mexico City, *Concr. Int. ACI* 8 (5) (1986) 23–36.
- [4] K. Kasai, B.F. Maison, Building pounding damage during the 1989 Loma Prieta earthquake, *Eng. Struct.* 19 (1997) 195–207.
- [5] Y.L. Xu, Q. He, J.M. Ko, Dynamic response of damper-connected adjacent buildings under earthquake excitation, *Eng. Struct.* 21 (1999) 135–148.
- [6] A.V. Bhaskararao, R.S. Jangid, Seismic response of adjacent buildings connected with friction dampers, *Bull. Earthq. Eng.* 4 (2006) 43–64.
- [7] S.E.A. Raheem, Mitigation measures for earthquake induced pounding effects on seismic performance of adjacent buildings, *Bull. Earthq. Eng.* 12 (2014) 1705–1724.
- [8] Z. Yang, X.L. Xu, X.L. Lu, Experimental seismic study of adjacent buildings with fluid dampers, *J. Struct. Eng. (ASCE)* 129 (2003) 197–205.
- [9] M. Basili, M. De Angelis, Optimal passive control of adjacent structures interconnected with nonlinear hysteretic devices, *J. Sound Vib.* 301 (2007) 106–125.
- [10] J. Kim, J. Ryu, L. Chung, Seismic performance of structures connected by viscoelastic dampers, *Eng. Struct.* 28 (2006) 183–195.
- [11] E.C. Kandemir-Mazanoglu, K. Mazanoglu, Parametric study on implementation of viscous dampers for adjacent buildings, *DSTA 2015 Conference Book: Dynamical Systems – Mechatronics and Life Sciences*, 2015, Vol. 2, pp. 313–322.
- [12] Federal Emergency Management Agency, NEHRP Guidelines for the Seismic Rehabilitation of Buildings, Rep. No. 273/274, Building Seismic Safety Council, Washington, D.C. 1997.
- [13] Federal Emergency Management Agency, Prestandard and Commentary for the Seismic Rehabilitation of Buildings, FEMA 356, Washington D.C. 2000.
- [14] M.D. Symans, M.C. Constantinou, Passive fluid viscous damping systems for seismic energy dissipation, *J. Earthq. Technol. ISET* 35 (4) (1998) 185–206.
- [15] R. Jankowski, Non-linear viscoelastic modelling of earthquake-induced structural pounding, *Earthq. Eng. Struct. Dyn.* 34 (2005) 595–611.
- [16] J.G.M. Van Mier, A.F. Puijssers, H.W. Reinhardt, T. Monnier, Load-time response of colliding concrete bodies, *J. Struct. Eng. (ASCE)* 117 (1991) 354–374.
- [17] Turkish Earthquake Code, Specification for structures to be built in disaster areas, Ministry of Public Works and Settlement, Government of Republic of Turkey, Ankara, 2007.